J Solid State Electrochem (2009) 13:1935–1944
DOI 10.1007/s10008-008-0742-9

ORIGINAL PAPER

Electrochemical nanogravimetric studies of sulfur/sulfide redox processes on gold surface

Elvira Bura-Nakic · András Róka · Irena Ciglenecki · György Inzelt

Received: 19 August 2008 / Revised: 5 November 2008 / Accepted: 7 November 2008 / Published online: 3 December 2008

Abstract Electrochemical quartz crystal microbalance, combined with cyclic voltammetric, chronoamperometric, and potentiostatic measurements, was used to study electrodeposition/dissolution phenomena at a gold electrode in solutions containing Na_2S. Spontaneous, open-circuit deposition processes as well as dissolution of the deposits in sulfide-free solutions have also been investigated. The potential range, scan rate, sulfide concentration, and pH have been varied. The results of the piezoelectric nanogravimetric studies are elucidated by a rather complex scheme involving underpotential deposition of sulfur at approximately −0.85 V vs. sodium calomel electrode, reductive dissolution of the deposited sulfur-containing layer at potentials more negative than approximately −0.9 V, and formation of a sulfur-containing multilayer at potentials more positive than −0.2 V. During the reduction of sulfur deposited on Au, a mass increase due to the formation of polysulfide species in the surface layer, accompanied by incorporation of Na^+ counterions, can be observed that starts at approximately −0.4 V. This is a reversible process, i.e., during the reoxidation, counterions leave the surface layers. Frequency excursions during the electroreduction and reoxidation processes reveal existence of several competitive dissolution–deposition steps. Spontaneous interaction between Au and HS^- species results in a surface mass increase at the open-circuit potential, and it also manifests itself in the substantial decrease of the open-circuit potential after addition of Na_2S to the supporting electrolyte.

E. Bura-Nakic (✉) · I. Ciglenecki
Department for Marine and Environmental Research,
Ruđer Bošković Institute,
Bijenička 54,
10000 Zagreb, Croatia
e-mail: ebnakic@irb.hr

A. Róka · G. Inzelt
Department of Physical Chemistry, Eötvös Loránd University,
Pázmány Péter sétány 1/A,
1117 Budapest, Hungary

G. Inzelt
e-mail: inzeltgy@chem.elte.hu

Introduction

The electrochemical reactions of sulfur and sulfur-containing compounds have been intensively studied in the last 30 years [1–19]. The intense interest arises mainly for three reasons: application of sulfur as a cathode material for high-energy density batteries, analysis of environmental samples, and modification of metal (mostly gold) surfaces by self-assembly of alkanethiols (RSH). The fundamental challenge concerning the formation of self-assembled monolayers is how to understand the nature of the bond between the gold surface and the thiol. There are different views in this respect: the explanation of the interaction between Au and S (HS^-) involves formation of a chemical bond (i.e., chemical reaction between Au and SH^- or RSH resulting in AuS or Au_2S), adsorption (van der Waals interactions), chemisorption by "partial charge transfer," etc.

We have encountered the problem of sulfur electrochemistry during our studies of sulfidic natural water samples. It became evident that it is impossible to understand the behavior of these systems containing metal sulfides without a detailed knowledge of the redox processes of sulfide and sulfur. Elucidation of the redox processes of sulfur and sulfides is a very difficult task for several reasons: e.g., formation of polysulfide ions in the solution and at the metal surface, the reactions between the metal and these species, and dependence of the equilibria and kinetics of the electrode processes on the nature of the contacting

solutions. Furthermore, there are contradictory views regarding the nature of the gold sulfides; beside Au_2S and Au_2S_3, AuS is also assumed. However, the latter might be a simple mixture of the previous two sulfides [20–25]. Although all the Au sulfides are insoluble in aqueous solutions—except under special conditions when the solution contains complexing agents (e.g., CN^- or concentrated Na_2S)—colloidal solution might be formed. It is also difficult to find a reliable value for the solubility product, which makes the adequate estimation of the standard (formal) potential of the respective electrode reaction uncertain. The solubility product of Au_2S was found smaller than that of the platinum metals, and it was established that K_{sp} is certainly not higher than 10^{-50} [20–22]. The recent and most reliable calculation [12] gives a value of pK_{sp}= 72.8 or pK_{sp}=55.5 when no strong base in high concentration is present since there are no S^{2-} ions in the solution. Taking into account the values of the dissociation constants of H_2S ($K_1=9.1\times10^{-8}$) and HS^- (many books and even recent papers, e.g., [4] reported value of $K_2=1.2\times10^{-12}$, while based on the results of careful spectroscopic and potentiometric studies a more acceptable value of approximately 10^{-17} [12, 16, 17, 23] was suggested), at pH=7 only H_2S and HS^- exist, while above pH=8 HS^- is dominating species. It follows that the formal potential of the S/SH^- system in neutral solutions is −0.4764 V, while in strongly acidic solution, it is −0.0624 V (earlier, for the S/S^{2-} system, a value of −0.447 V was the accepted standard potential; however, recently, −0.575 V was suggested [12]).

From the thermodynamical data, the standard potential of the electrode reaction

$$Au_2S + 2e^- \rightleftarrows 2Au + S^{2-} \quad (1)$$

is approximately −0.329 V vs. SHE (standard hydrogen electrode), i.e., it may occur spontaneously in the potential region where S^0/S^{2-} couple is usually studied since the standard potential of the latter couple is −0.447 V [19]. However, if AuS (a mixture of Au_2S and Au_2S_3) is considered, the equilibrium potential is approximately 0.03–0.04 V.

Previous studies have revealed that when Au is immersed in an electrolyte containing Na_2S, both the spontaneous processes (underpotential deposition of sulfide on Au and reaction between Au and S) and the potential-dependent redox reactions involve changes of the surface mass. Therefore, piezoelectric nanogravimetry with an electrochemical quartz crystal microbalance (EQCM) is an attractive choice to follow these surface events. A knowledge of the surface mass changes leads to a deeper understanding of the complex reaction mechanism of the oxidative deposition of sulfur and the reductive transformation and stripping of the surface sulfur layer.

In this work, we present results of EQCM investigations of the deposition and stripping of sulfur on gold in NaCl and NaCl–$NaHCO_3$ electrolyte solutions containing Na_2S. These electrolyte compositions are quite similar to those of the natural seawater samples. Therefore, besides obtaining new and important information concerning the events occurring during redox transformations of sulfur–sulfide system, these results could serve as a starting point for reliable electroanalysis of environmental samples.

Experimental

Six megaherz AT-cut crystals were used in the EQCM measurements. Each side of the crystal was coated with gold. The crystal was mounted in a suitable formed part of a holder made from Teflon that also contained the oscillator circuit which was isolated from the solution. Only one side of the crystal was exposed to the electrolyte solution. Connections to the metal coatings of both sides of the crystal were made with gold foil. The projected and piezoelectrically active area of the working electrode (A) was 0.4 cm^2. A Pt wire was used as a counter electrode. The reference electrode was a sodium chloride saturated sodium calomel electrode (SCE). The Sauerbrey equation was used for estimation of the surface mass changes (Δm) from the frequency changes (Δf), with an integral sensitivity, $C_f=8.15\times10^7$ Hz cm^2 g^{-1}, that was determined in separate experiments [26].

$Na_2S\cdot9H_2O$ sulfide stock solutions were prepared in deionized water which was purged with Ar prior to addition of $Na_2S\cdot9H_2O$ crystals. All solutions were purged with Ar throughout the experiments. An Elektroflex 453 potentiostat and a Universal Frequency Counter TR-5288 connected with an IBM personal computer were used for the control of the measurements and for the acquisition of the data. Electrolyte solutions used were 0.55 M NaCl, 0.55 M NaCl and 0.03 M $NaHCO_3$ (pH=8.5) containing Na_2S in different concentrations from 7×10^{-6} up to 1.54×10^{-3} M.

Results and discussion

Cyclic voltammetric EQCM study of sulfide/gold system. The starting potential for voltammograms shown in Fig. 1 was set at −1.1 V where a clean Au surface is expected since no sulfur is supposed to be deposited in this potential range [1–9]. The only electrode process occurring is hydrogen evolution reaction (HER). According to the literature, [1–9] an underpotential deposition (UPD) of sulfur occurs at approximately −0.9 V vs. SCE, and indeed a small anodic wave (A1) appeared in the voltammograms that was accompanied with a minor frequency decrease.

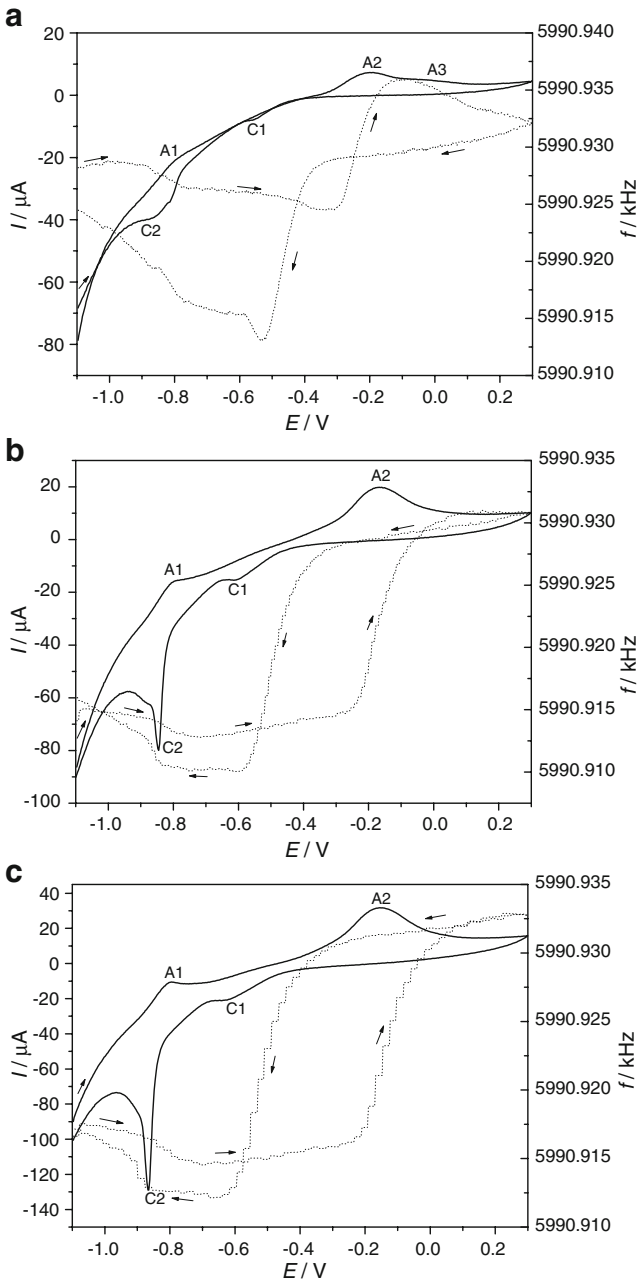

Fig. 1 Cyclic voltammograms (*solid line*) and corresponding frequency changes (*dotted line*). Electrolyte: 3.5×10^{-4} M Na_2S in 0.55 M NaCl solution, pH=7. Starting potential: −1.1 V. Scan rates: **a** 5, **b** 25, and **c** 50 mV s^{-1}

This mass increase corresponds to approximately 7×10^{-10} mol S cm^{-2} which indicates the formation of a sulfur monolayer. There have been several studies that intended to clarify the exact nature of the UPD process and the surface species formed. According to the scanning tunneling microscopy (STM) results, polymeric S species (S_n) are formed on the surface. However, the state, i.e., the *n* value, the distribution of the species, and even the actual valency of sulfur, was shown to be strongly dependent on the potential, sulfide concentration, and pH of the contacting solution [7]. According to electron spectroscopy for chemical analysis, Raman, and Surface-Enhanced Raman Scattering spectra [1, 3, 6–8], S^0, S_2^{2-}, and S^{2-} can be detected on the surface; and "strong bonding" between Au atoms and sulfur, followed by the formation of gold-sulfide, has been assumed [1, 2, 4, 6–9].

The mass increase measured by nanogravimetry supports the explanation that the following reactions take place [2]:

$$\mathrm{Au} + \mathrm{SH}^- \rightarrow \mathrm{Au} - (\mathrm{SH}^-)_{\mathrm{ads}} \tag{2}$$

$$\mathrm{Au} - (\mathrm{SH}^-)_{\mathrm{ads}} \rightarrow \mathrm{Au} - \mathrm{S} + \mathrm{H}^+ + 2\mathrm{e}^- \tag{3}$$

As seen in Fig. 1, neither the main characteristics of the cyclic voltammogram nor the mass excursion depend on the scan rate. However, at potentials more positive than E_p (A1), there are certain differences which attest that kinetics is also involved.

The second characteristic anodic peak appears at approximately −0.2 V which has been assigned to the electrodeposition of S^0 due to the oxidation of HS^- ions which eventually results in a sulfur multilayer assuming a reaction scheme as follows [2, 3]:

$$\mathrm{Au} - \mathrm{S} + x\mathrm{HS}^- + x\mathrm{OH}^- \rightarrow (\mathrm{AuS})\left(\mathrm{S}_x^{2-}\right) + x\mathrm{H_2O} + 2(x-1)\mathrm{e}^- \tag{4}$$

$$(\mathrm{Au} - \mathrm{S})\left(\mathrm{S}_x^{2-}\right) \rightarrow (\mathrm{Au} - \mathrm{S})\left(\mathrm{S}_x^{0}\right) + 2\mathrm{e}^- \tag{5}$$

Based on the results of modulated reflectance spectroscopy [2] and rotating ring disc electrode studies [1], the formation of soluble polysulfides by a chemical reaction of the deposited S^0 and SH^- ions has also been suggested:

$$(\mathrm{Au} - \mathrm{S})\left(\mathrm{S}_x^{0}\right) + \mathrm{SH}^- \rightarrow (\mathrm{Au} - \mathrm{S})\left(\mathrm{S}_{x-n}^{0}\right) + \mathrm{S}_{n+1}^{2-} + \mathrm{H}^+ \tag{6}$$

The latter effect has to be sensitive to the scan rate since the surface mass change is a result of two competitive processes, oxidation of sulfide which results in the deposition of sulfur, and the chemical reaction between deposited S and HS^- from the solution. The rate of the latter process depends on rates of the diffusion of HS^- ions and the chemical reaction. However, the situation is more complicated; at wave A2, always a frequency increase (mass decrease) is observed that is followed by a mass increase at higher positive potentials. At more positive potentials—depending on the scan rate—another, less developed oxidation wave (peak A3 in Fig. 1a) appears at which the deposition starts. This does not mean that the formation and deposition of S^0 would not start at more

negative potentials; the open-circuit and potentiostatic investigations clearly reveal deposition in this potential interval as well (see later). Of course, we may assume that, in the first phase of electrooxidation of the surface layer, the formation of soluble polysulfides takes place, and—which has been neglected so far—counterions also leave the surface layer as it loses its negative charges. Assuming a layer of finite thickness not just a monolayer, the following equation is operative:

$$(\mathrm{Au-S})\left(\mathrm{S}_x^{2-}\mathrm{Na}_2^+\right) \rightarrow (\mathrm{Au-S})\left(\mathrm{S}_x^0\right) + 2\mathrm{e}^- + 2\ \mathrm{Na}^+ \quad (7)$$

However, in this way it cannot be explained that the frequency value is higher at −0.2 V than at −1.1 V. Therefore, it should be assumed that, at −1.1 V, the deposited layer was not perfectly removed even if the electrode was held at this potential for several minutes before starting the cycle. If this argument is valid, the UPD can occur only at the free sites of the gold surface. Alternatively, we may assume the dissolution of the gold sulfide during the electrooxidation, which is also thermodynamically possible. Surprisingly, this process has not been taken account so far, while it seems to be rather plausible once the formation of Au_2S or AuS has been predicted. Therefore, we would propose the following reaction:

$$\mathrm{Au_2S} \rightarrow 2\mathrm{Au}^+ + \mathrm{S} + 2\mathrm{e}^- \quad (8)$$

From the detected frequency increase at peak A2, the dissolution of $\Gamma=5\times10^{-10}$ mol gold-atom cm^{-2} can be derived, which is a reasonable value taking into account the calculated surface concentration of S after the UPD process. It may be assumed that most Au^+ ions are redeposited due to the fast reaction:

$$2\mathrm{Au}^+ + \mathrm{HS}^- \rightarrow \mathrm{Au_2S} + \mathrm{H}^+ \quad (9)$$

A part of the Au^+ ions can diffuse into the solution phase which is supported by the observation that, after intensive use of the gold-coated crystals in some cases, a permanent mass loss was observed. This explanation is reasonable, but in the potential region between −0.2 and −0.6 V, the mass change is reversible during oxidation–reduction (see Fig. 1), which is certainly inconsistent with the irreversible dissolution of gold.

Although the main features of the voltammograms and the EQCM responses are practically the same, the reduction cycle is influenced by the scan rate (Fig. 1a–c). The scan rate is found to be related to the time that the system spends at positive potentials where the oxidation of sulfide and the formation of sulfur layer can occur. Under the conditions applied during cycling even at slow sweep rates, the deposition is not too intensive (at 5 mV s^{-1}, it is approximately 5 Hz, while at 50 mV s^{-1}, it is practically zero). Two waves appear in the course of the negative-going cycle which have been observed in several studies earlier [1–4]. The peak labeled here as C1 has usually been assigned to the electroreduction of the sulfur multilayer to polysulfide species, while the peak labeled C2 has been assigned to the reduction of polysulfides to sulfide and the reduction of the AuS which formed during the UPD process [We avoided the usual notation (A1–C1, A2–C2 pairs) and just labeled the anodic peaks as A1, A2, and A3 and cathodic peaks as C1 and C2 in order of their appearance in the course of the oxidation and reduction, respectively, because these peaks are not entirely corresponding redox couples]. However, the EQCM curves reveal that the situation is more complicated. At A2, mostly dissolution (mass loss) occurs, and the deposition starts at A3, while an increase of the surface mass begins at more positive potentials than could be related to C1 if it were a simple reduction process. At C1, a rather complicated deposition–dissolution pattern arises according to the EQCM curves. At C2, a mass loss can be observed, which supports the previous views, i.e., the formation of soluble sulfide species that leave the surface.

The cyclic voltammetric experiments were also carried out by using starting potentials in the potential region where the oxidation of HS^- ions occurs and the deposition of sulfur multilayer is expected. The cyclic EQCM curves were taken at different starting potentials, different waiting times and potential ranges, scan rates, and concentrations. In some experiments, $NaHCO_3$ was also added to buffer the solutions, even though no substantial pH effect was observed attesting to the self-buffering ability of the sulfide system. The measured pH was always between pH=8 and 10. Selected typical results are shown in Fig. 2.

The cyclic voltammetric responses are basically similar in as much as the typical peaks appear and the peak potentials practically do not change, independently of the variation of the parameters such as scan rate, starting potential, and waiting time, while the EQCM responses are substantially different. In Fig. 2a, the low starting frequency indicates the accumulation of a sulfur layer while holding the potential at 0.3 V for 15 s. As has already been discussed, a mass gain can be observed before peak C1, and in the region of C1, a dissolution–deposition pattern can be seen on the EQCM curve. Starting at the second main reduction step, a dissolution occurs. A small mass increase can be observed again at A1, while a dissolution starts before A2 which is followed by a deposition. Figure 2b shows that at higher scan rate there is no dissolution during the negative-going scan. Dissolution starts only at the beginning of the positive-going scan. After A1 is reached, the mass increase can be detected again. The mass loss starts at A2, and due to the fast scan rate and less positive end-potential, no deposition occurs until the end of the

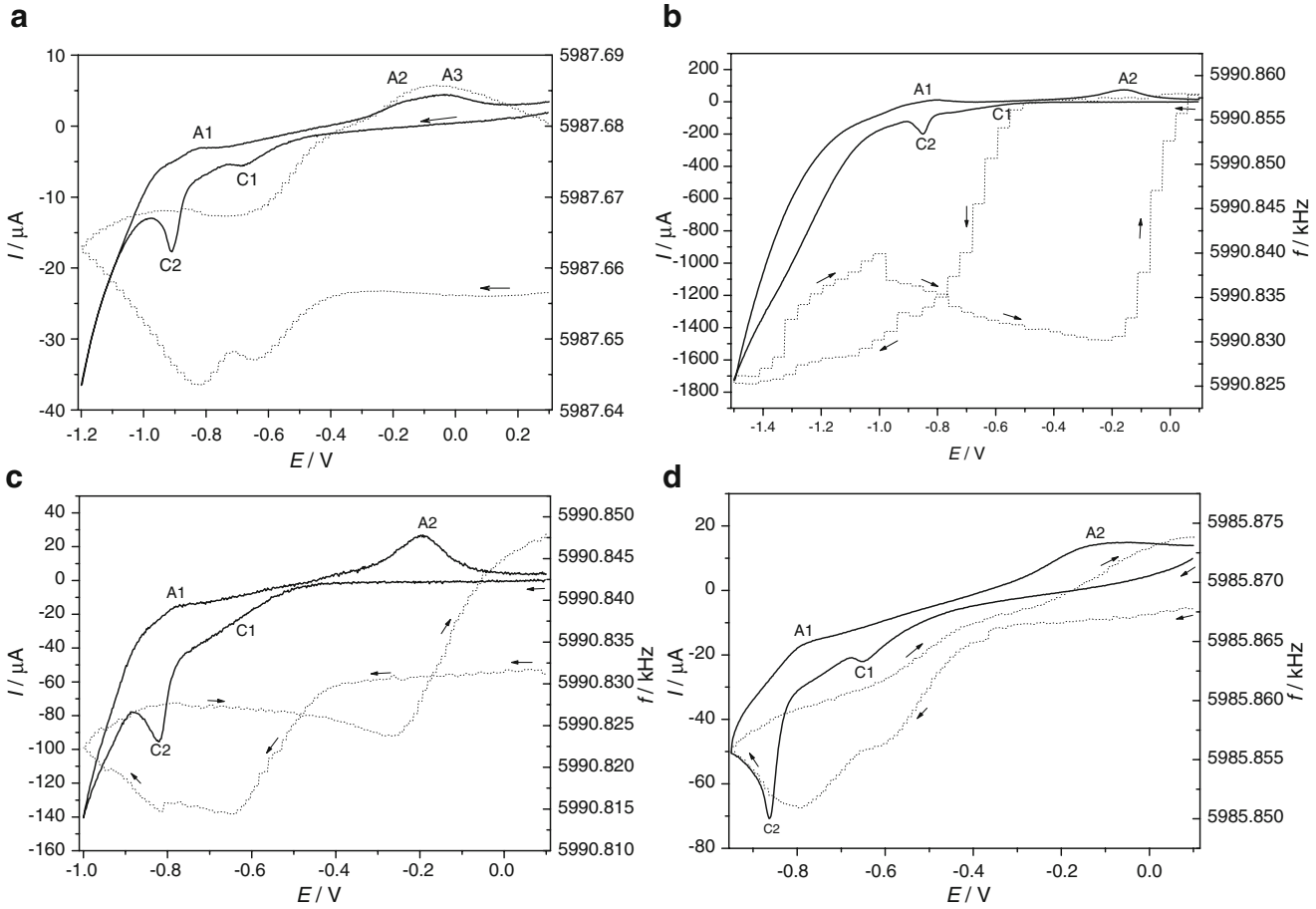

Fig. 2 Cyclic voltammograms (*solid line*) and corresponding frequency changes (*dotted line*). Electrolyte: **a** and **d** 6.6×10^{-4} M, **b** and **c** 1.5×10^{-3} M Na_2S in 0.55 M NaCl solution. In the case of **b** and **c**, the solution also contained 3×10^{-2} M $NaHCO_3$. pH 7. Starting potentials: **a** 0.3 V, **b**–**d** 0.1 V. Scan rates: **a** 50, **b** 100, **c** and **d** 25 mV s^{-1}. Waiting times at the starting potentials: **a** and **d** 15 s, **b** and **c** 30 s

cycle. However, the deposition of sulfur multilayer takes place at 0.1 V.

The curves in Fig. 2c show the next cycle taken after that shown in Fig. 2b while holding the electrode at 0.1 V for 30 s. It can be seen that the initial frequency value is less by 27 Hz. Albeit the scan rate was only 25 mV s^{-1}, the perfect removal of the surface layer did not take place during reduction, but a substantial part of it was removed during oxidation at peak A2. Experiments have been carried out by gradually applying a less negative switching potential in order to make sure that hydrogen evolution was not affecting the EQCM response. As seen in Fig. 2d, there was no effect of the HER on the response.

Chronoamperometric-potentiostatic experiments

Because the results of the cyclic voltammetric experiments revealed several fast and slow follow-up processes, potential step experiments seemed to be a plausible choice to gain a better understanding of these processes.

As seen in Fig. 3a, when Na_2S was added to the supporting electrolyte, a substantial −300 mV decrease of the rest potential was observed, which indicates a reaction between Au and HS^- ions according to Eqs. 2 and 3 (In fact, sulfur-modified Au-S electrodes were prepared in this way [13]). Adjusting the same pH by adding NaOH caused a much less change of the open-circuit potential than was observed in the presence of Na_2S. Rather surprisingly, the frequency decrease indicates a surface coverage that is higher than would correspond to a monolayer since 25 Hz is approximately equal to 9.8×10^{-9} mol S cm^{-2}. After a short induction period, the spontaneous deposition is rather fast, and at longer times, there is still a frequency decrease albeit in a rather slow rate. Both the supporting electrolyte and the Na_2S solution were carefully purged by Ar gas. Nonetheless, it cannot be excluded that a spontaneous oxidation of HS^- ions by the still remaining oxygen occurs. At the same time, it is less likely that the resulting S^0 will be deposited on the gold surface. The decrease of the rate of the deposition is also against this explanation. It is most

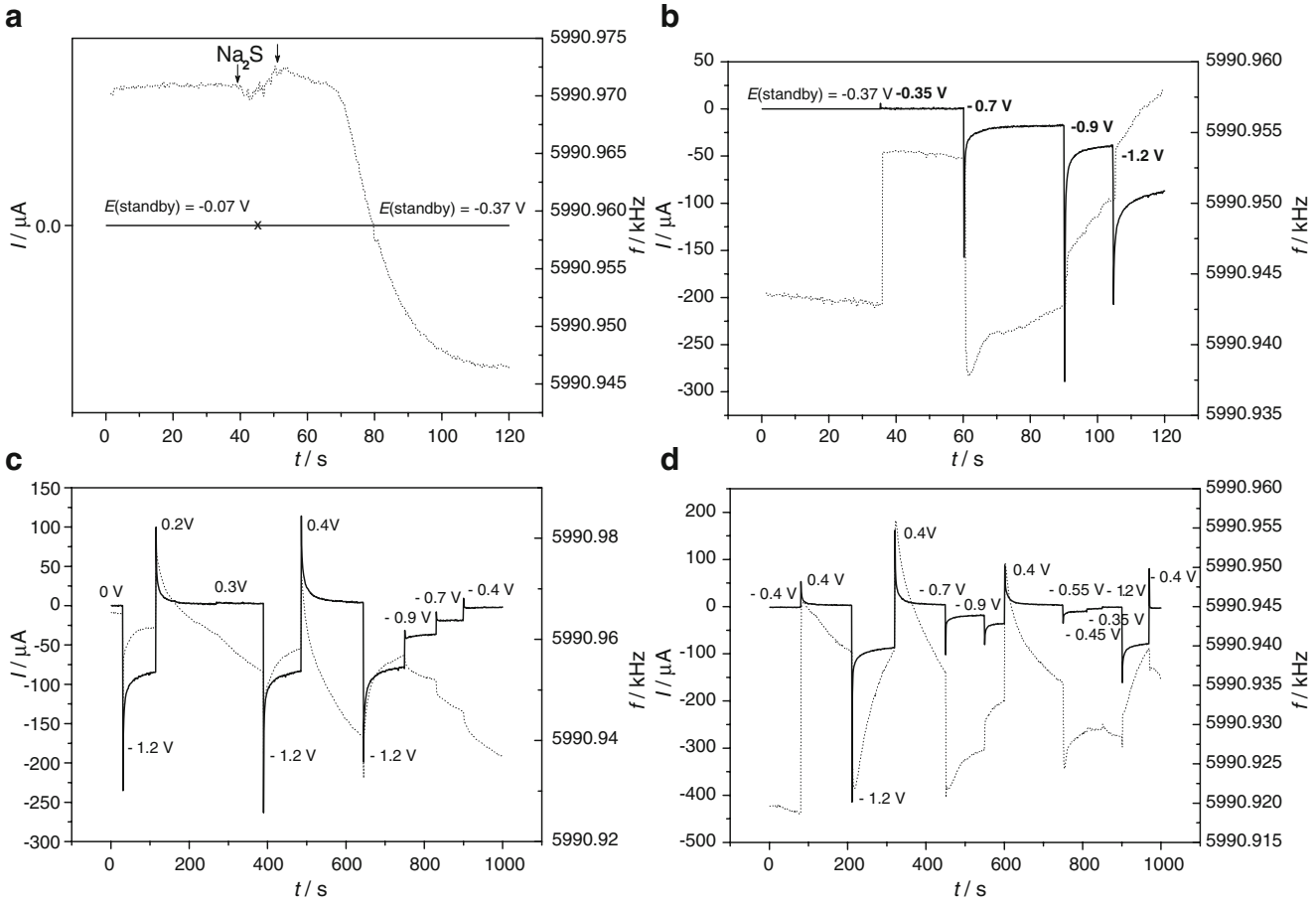

Fig. 3 Open-circuit and potential step experiments. Current (*continuous line*) and simultaneously obtained EQCM frequency responses (*dotted line*). **a** Open-circuit experiments. Na_2S solution was added to the solution of 0.55 M NaCl at the time indicated by an *arrow*. The *second arrow* indicates the end of the stirring after mixing. The final concentration of Na_2S was 6×10^{-4} M. **b**–**d** Consecutive cathodic and anodic potential steps as indicated in the figure

likely that, after the formation of the first layer, which is Au_2S, additional sulfur-containing layers are formed. Just a +20 mV potential step from the open-circuit potential results in fast and substantial frequency increase (Fig. 3b second section). The next step to −0.7 V, where on the cyclic voltammograms two frequency "peaks" appeared (Figs. 1 and 2), results in a more complex frequency response: first, a large frequency decrease, then a fast frequency increase develop, while eventually the resultant response is a slow-frequency increase. Stepping to −0.9 V results in a intense dissolution, which continues with an even higher rate at −1.2 V. When the potential was stepped from 0.0 V to −1.2 V, another interesting response can be detected (Fig. 3c). First, a frequency decrease, then a fast frequency increase, occur. In accordance with the cyclic voltammetry-EQCM results, this can be explained by the formation of insoluble polysulfides and the incorporation of Na^+ counterions into the layer, then the dissolution of the product from the further electroreduction. The dissolution slows down, which is an explanation why, in the case of cyclic voltammograms, the reductive desorption has not been completed within the time scale of the experiments. This remaining layer can be removed by oxidation with a potential step to 0.2 V. At 0.2 V, and even more intensively at 0.3 V, deposition also takes place as it has already been discussed for the cyclic voltammetry-EQCM responses. Similar deposition–dissolution behavior can be observed again during the potential step from 0.3 to −1.2 V. During the next oxidation step, first, a mass decrease then a rather fast mass increase occurs at 0.4 V. Stepping to −1.2 V again, the response described previously develops, but by applying steps with smaller amplitude in the direction of less negative potentials, deposition can be monitored as in Figs. 1 and 2b–d. The layer deposited at −0.4 V can be removed by oxidation at 0.4 V, where deposition starts again (Fig. 3d). Stepping again to −1.2 V, a fast mass increase then a decrease can be observed, and stepping back to 0.4 V, the previously described phenomenon was observed again. The step from 0.4 to

−0.7 V results in the complex EQCM response which has already been shown in Fig. 3b attesting the excellent reproducibility of the measurements. The similar statement is valid to the further responses presented in Fig. 3d.

Figure 4 shows the responses of two steps in a longer time scale. At 0.3 V, a continuous deposition occurs which can be related to the formation of a sulfur multilayer. By stepping to −0.7 V, first a fast deposition, then a dissolution occurs (Fig. 4a). When the potential is stepped from −0.3 to −0.7 V, first a fast deposition then a fast dissolution occurs (Fig. 4b). In principle, the piezoelectric nanogravimetry technique by using EQCM provides information on electrochemical equivalent (the apparent molar mass, M_{app}) of the deposited or exchanged species knowing the frequency change and the corresponding charge consumed. Unfortunately, in this case, reliable quantitative data can be obtained only concerning the amount of the deposited material beside the qualitative information on the deposition–dissolution processes because a substantial amount of charge is consumed by redox processes in which both the reactant and the products are soluble, i.e., no change of the surface mass occurs. In this way, rather small M_{app} values can be calculated since it is proportional to $\Delta f/Q$. Furthermore, chemical reactions are also involved which lead to spontaneous dissolution–deposition processes. For instance, from the curves shown in Fig. 4a, in the case of deposition M_{app}=6.5, while for the dissolution M_{app}=13 g mol^{-1} can be derived.

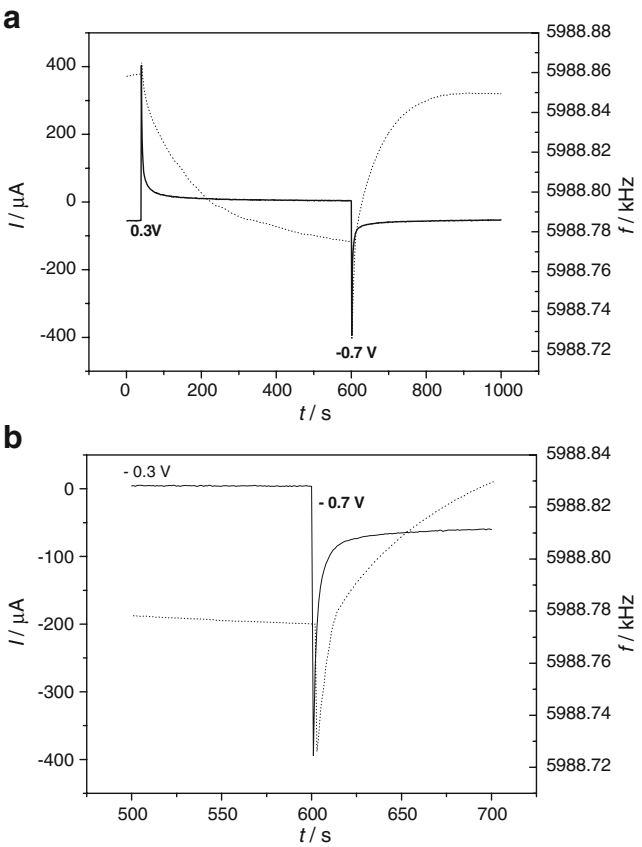

Fig. 4 Chronoamperometric QCM curves obtained by potential steps **a** from 0.3 to −0.7 V and **b** from −0.3 to −0.7 V for Au electrode immersed in 0.55 M NaCl and 3.2×10^{-4} M Na_2S solution

M_{app}=6.5 could be assigned to the process described by Eq. 4 assuming a multicharged polysulfide as follows:

$$\mathrm{Au-S}+x\mathrm{HS}^- + x\mathrm{OH}^- \rightarrow (\mathrm{AuS})\left(\mathrm{S}_x^{2y-}\right) + x\mathrm{H_2O} + 2(x-y)\mathrm{e}^- \quad (10)$$

or

$$\mathrm{Au-S}+5\mathrm{HS}^- + \mathrm{OH}^- \rightarrow (\mathrm{AuS})\left(\mathrm{S}^0\right)\left(\mathrm{HS}^-\right)_{4(\mathrm{ads})} + \mathrm{H_2O} + 2\mathrm{e}^- \quad (11)$$

Nonetheless, it is not unimaginable that sorption of HS^- ions is enhanced by the deposition of sulfur, M_{app}=6.5 would mean that the ratio of charged and uncharged sulfur is 4:1 which is less likely.

It is more reasonable to assume that partially charged polysulfides dissolve.

We encountered similar problems also when we calculated M_{app} values from the different sections of cyclic voltammograms or chronoamperometric curves. In the region of HER, it can easily be explained by the charge consumed by hydrogen evolution. However, there was one section where always reasonable M_{app} values were obtained which was close to the molar mass of sodium ion, that is, the mass increase that usually starts around −0.4 V, which is at more positive potentials than the peak potential of C1, and ends around E_p(A1) during the negative-going scans. If our assumption were correct, i.e., during the reduction of the sulfur layer in the first phase, insoluble polysulfides would be formed, and the mass increase would be related to the incorporation of the charge-compensating counter cations. The same effect must be observed even in the case when a deposited sulfur layer is reduced in a supporting electrolyte which does not contain HS^- ions. The results of such an experiment shown in Fig. 5 fulfill these expectations.

Somewhat surprisingly in this case, C1 is absent or at least it does not appear as a well-developed peak. A similar observation was made when the scan was started from negative potentials falling in the range of −0.2 and −0.4 V, especially when it was the first cycle after the addition of Na_2S. From the curves presented in Fig. 5, for the interval between −0.6 and −0.8 V, M_{app}=28 g mol^{-1} can be calculated. Therefore, the dominating process in this region is as follows:

$$(\mathrm{Au-S})\left(\mathrm{S}_x^0\right) + 2\mathrm{e}^- + 2\mathrm{Na}^+ \rightarrow (\mathrm{Au-S})\left(\mathrm{S}_x^{2-}\mathrm{Na}_2^+\right) \quad (12)$$

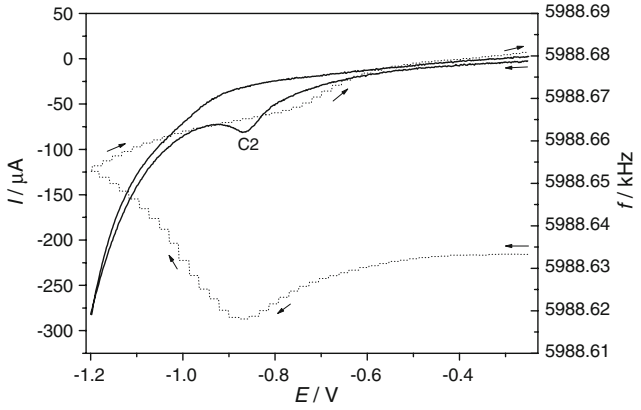

Fig. 5 The cyclic voltammogram (*solid line*) and the corresponding frequency-potential curve (*dotted line*) obtained for an AuS-(S_x) electrode in contact with 0.55 M NaCl at a scan rate of 50 mV s^{-1}

considered. The increase of the Na_2S content in the unbuffered solution increases the pH of the solution, and consequently, the ratio of HS^-/H_2S is also shifted. The reduction of polysulfide to sulfide at C2 that leads to dissolution of the layer can be described as follows:

$$\mathrm{AuS}\left(\mathrm{S}_x^{2-}\right) + 2xe^- + (x+1)\mathrm{H}^+ \rightarrow \mathrm{Au} + (x+1)\mathrm{HS}^- \tag{13}$$

According to Eq. 13, as the pH increases, a negative shift of the peak potential has to be observed. The increase of the peak current is related to the amount of sulfur attached to the gold surface. As seen in Fig. 6b, the starting frequency is lower when the sulfide concentration is higher which also indicates that both the spontaneous and the electrochemically induced (at 0.3 V) depositions—as expected—are

The effect of the sulfide concentration on the cyclic EQCM response

The cyclic voltammograms and the simultaneously detected EQCM frequency responses obtained at three different Na_2S concentrations are displayed in Fig. 6.

In all solutions, the characteristic peaks of the cyclic voltammetry appear, and they are getting more and more pronounced with increasing concentrations of sulfide (C1 is practically missing in the most dilute solution which may be related to the observation that no polysulfide formation takes place in such solutions [7, 8]). The EQCM curves are similar to those presented earlier, only herein the reduction in the potential range below −0.8 V, and the removal of the surface layer were practically completed. All voltammetric peaks are shifted into the direction of more negative potentials with increasing concentrations of sulfide by 180 (C1), 58 (C2), 60 (A1), and approximately 120 (A2) mV $decade^{-1}$. Based on these rather uncertain values, only qualitative conclusions can be drawn. The error of the values given is as high as 15 mV. Especially the overlapping of A2 and A3 waves allows no more accurate calculations. We have tried to utilize the EQCM curves shown in Fig. 6b in such a way that E_p (A2) was determined from the place of the maximum slope of the frequency increase between approximately −0.22 and −0.1 V (curves 2 and 3 of Fig. 6b), since at A2, dissolution takes place. Since it is assumed that, in the reactions C1 and C2, the deposited sulfur (polymeric sulfur) and the polysulfides formed in step C1, respectively, participate, no shift is expected without assuming that one of the components of the solution also takes part in the electrochemical process. Because the concentration of sodium ions is constant, the role of HS^- and H^+ or OH^- ions has to be

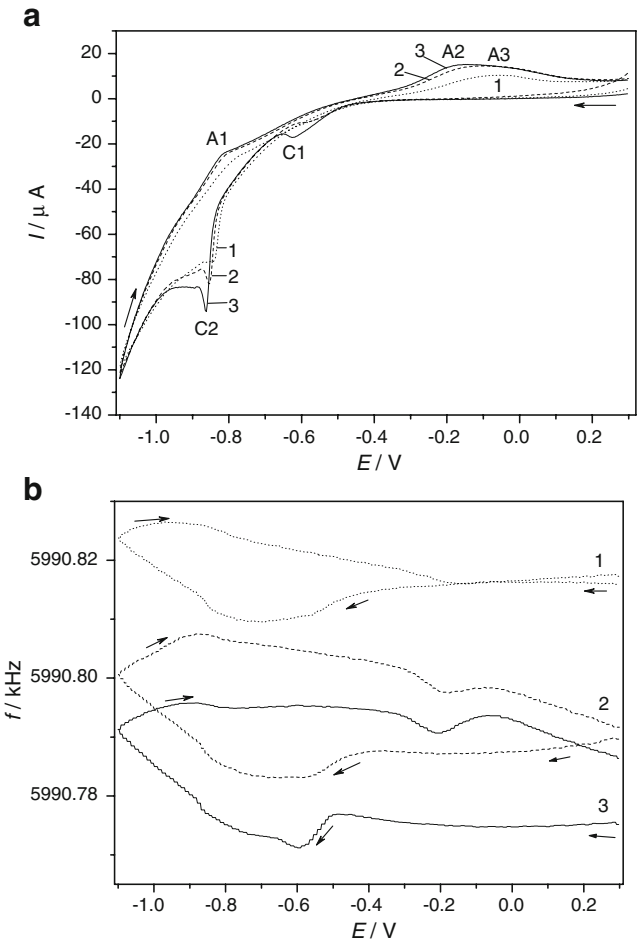

Fig. 6 Cyclic voltammograms (**a**) and the simultaneously detected EQCM frequency responses (**b**) obtained at three different Na_2S concentrations: (*1*) 1.8×10^{-4}, (*2*) 5.2×10^{-4}, and 8.4×10^{-4} M Na_2S. The respective pH values are (*1*) 9.0, (*2*) 9.7, and (*3*) 9.96. Scan rate, 25 mV s^{-1}. Supporting electrolyte, 0.55 M NaCl

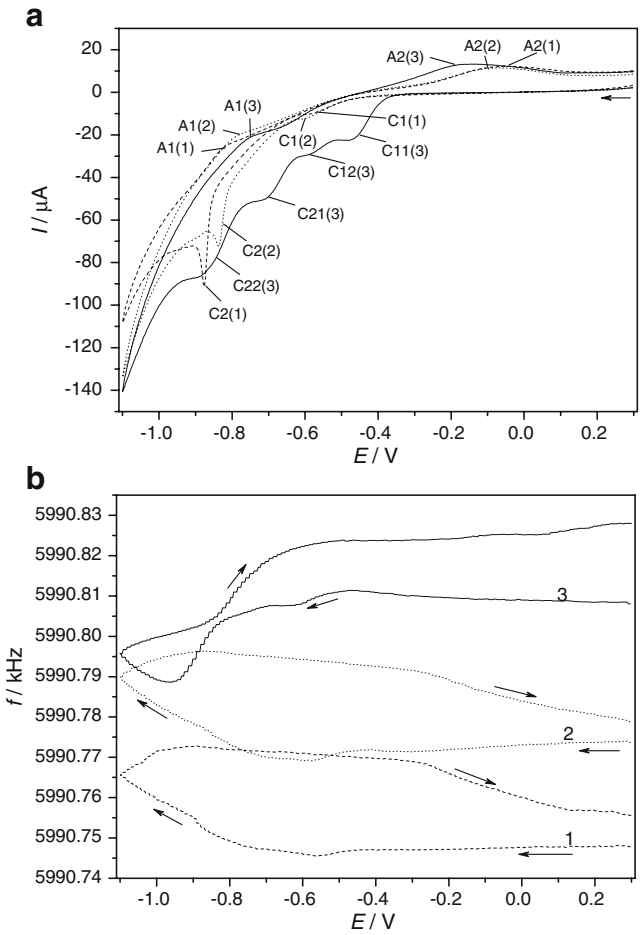

Fig. 7 Cyclic voltammograms (**a**) and the simultaneously detected EQCM frequency responses (**b**) obtained at three different pH values: (*1*) 10.2, (*2*) 8.0, and (*3*) 3.2. The pH was adjusted by adding HCl or NaOH to the solution containing 0.55 M NaCl and 8.4×10^{-4} M Na_2S. Scan rate: 25 mV s^{-1}

faster when the gold substrate is in contact with a more concentrated Na_2S solution. In order to check the effect of pH, experiments at three different pH values have also been carried out. Fig. 7 shows the cyclic EQCM curves obtained at pH=3.2, 8.0, and 10.2, respectively.

All the peaks—as in the case of the concentration effect described above—shift in the direction of the negative potentials with increasing pH. The negative potential shift with increasing pH is well seen also for the background current due to HER. At pH=8 and 10.2, the shape of the voltammetric curves and the main features of the EQCM response remain the same. The shift in the anodic peak potentials is related to both the concentration of the HS^- ions and the H^+ (OH^-) ions according to Eqs. 2–5, 10, and 11. At lower pH values, drastic changes can be observed. It is related to the presence of H_2S since at pH and approximately <5.5, only this protonated form exists in the solution. At pH=3.2, both C1 and C2 split into two waves (labeled as C11, C12 and C21, C22, respectively). Under identical conditions, less sulfur was deposited at 0.3 V (see Fig. 7b). At wave C11 is a slight mass decrease, while at C12 a mass increase occurs, and at both C21 and C22 a mass increase takes place. The dissolution starts only during the positive-going scan. At the end of the cycle (after A2), no deposition occurs as in the case of higher pHs. It means that A3 is shifted to more positive potentials.

Conclusions

The results of the open-circuit, cyclic voltammetric, and potential step quartz crystal microbalance experiments attest that the electrochemical transformations occurring in aqueous solution of Na_2S at a gold electrode is more complex than has been thought.

The potential-dependent surface mass changes observed are in accordance with the previous views regarding the following processes: underpotential deposition of sulfur species at the potential of approximately −0.8 V vs. SCE, formation of sulfur multilayer above approximately −0.2 V in basic solutions, formation of polysulfides during reduction between −0.4 and −0.8 V, and removal of the surface layer due to the complete reduction to HS^- species. However, several other processes take place during both electrooxidation and electroreduction. During electrooxidation at approximately −0.3 V, a fast dissolution occurs due to the formation of soluble polysulfides, which process competes with the deposition of a sulfur multilayer. In the course of the reduction, first insoluble polysulfides are formed which are accompanied by incorporation of Na^+ counterions into the surface layer. In the potential region of −0.5 and −0.85 V, several competitive processes take place which result in a rather complex dissolution–deposition behavior. The addition of Na_2S into the supporting electrolyte causes a approximately −300 mV decrease of the rest potential indicating a strong interaction between the gold substrate and HS^- ions which results in the formation of gold-sulfide. At the open-circuit potential, further deposition can be detected which is related to the adsorption of HS^- species.

The pH dependence can be explained by the ratio of HS^- and H_2S present in the solution, e.g., the participation of H^+ ions in the reaction of sulfur reduction.

Acknowledgment This work is supported by bilateral program cooperation between Republic of Croatia and Hungary CRO-01/2006 as well as by national research projects no. 098-0982934-2717 from the Ministry of Science and Technology of the Republic of Croatia (IC and EB-N) and OTKA K71771 from the National Scientific Research Fund, Hungary (GI).

References

1. Buckley AN, Hamilton IC, Woods R (1987) J Electroanal Chem 216:213. doi:10.1016/0022-0728(87)80208-5
2. Lezna RO, de Tacconi NR, Arvia AJ (1990) J Electroanal Chem 283:319. doi:10.1016/0022-0728(90)87398-4
3. Gao X, Zhang Y, Weaver MJ (1992) Langmuir 8:668. doi:10.1021/la00038a060
4. Parker GK, Watling KM, Hope GA, Woods R (2008) Colloids Surfaces A 18:151. doi:10.1016/j.colsurfa.2007.12.029
5. Quijada C, Huerta FJ, Morallón E, Vázquez JL, Berlouis LEA (2000) Electrochim Acta 45:1847. doi:10.1016/S0013-4686(99)00396-5
6. Vericat C, Vela ME, Andreasen G, Salvarezza RC, Vazquez L, Martin-Gao JA (2001) Langmuir 17:4919. doi:10.1021/la0018179
7. Vericat C, Vela ME, Gago J, Salvarezza RC (2004) Electrochim Acta 49:3643. doi:10.1016/j.electacta.2004.02.046
8. Lay MD, Varazo K, Stickney JL (2003) Langmuir 19:8416. doi:10.1021/la034474y
9. Biener MM, Biener J, Friend CM (2005) Langmuir 21:1668. doi:10.1021/la047387u
10. De Tacconi NR, Rajeshwar K (1998) J Electroanal Chem 444:7. doi:10.1016/S0022-0728(97)00533-0
11. Myung N, Kim S, Lincot D, Lepiller C, de Tacconi NR, Rajeshwar K (2000) Electrochim Acta 45:3749. doi:10.1016/S0013-4686(00)00472-2
12. Licht S (1988) J Electrochem Soc 135:2971. doi:10.1149/1.2095471
13. Hepel M, Janusz W (2000) Electrochim Acta 45:3785. doi:10.1016/S0013-4686(00)00468-0
14. Zhdanov SI (1982) Sulfur. In: Bard AJ (ed) Encyclopedia of electrochemistry of elements, vol. 6. Marcel Dekker, New York, p 273
15. Zhdanov SI (1985) Sulfur, selenium, tellurium, and polonium. In: Bard AJ, Parsons R, Jordan J (eds) Standard potentials in aqueous solution. Marcel Dekker, New York, p 93
16. Levillain E, Demortier A, Lelieur J-P (2006) Sulfur. In: Scholz F, Pickett CJ (eds) Inorganic electrochemistry, Bard AJ, Stratmann M (eds) Encyclopedia of electrochemistry, vol 7a. Wiley-VCH, Weinheim, p 253
17. Orlik M, Galus Z (2006) Electrochemistry of gold. In: Scholz F, Pickett CJ (eds) Inorganic electrochemistry. Bard AJ, Stratmann M (eds) Encyclopedia of electrochemistry, vol 7b. Wiley-VCH, Weinheim, pp 853–854
18. Inzelt G (2006) Standard, formal, and other characteristic potential of selected electrode reactions. In: Scholz F, Pickett CJ (eds) Inorganic electrochemistry, Bard AJ, Stratmann M (eds) Encyclopedia of electrochemistry, vol 7a. Wiley-VCH, Weinheim, pp 64–66
19. Schmid GM (1985) Gold. In: Bard AJ, Parsons R, Jordan J (eds) Standard potentials in aqueous solution. Marcel Dekker, New York, p 313
20. Busev AI, Ivanov VI (1973) Analytical chemistry of gold. Nauka, Moscow, p 28 (in Russian)
21. Peschevskii BI, Anoshin TN, Ehrenburg AM (1965) Dokl AN USSR 162:915
22. Cherneva AN (1960) Trudi Uralskogo Polytech Inst 96:134
23. Morris T, Copeland H, Szulczewski G (2002) Langmuir 18:535. doi:10.1021/la011186y
24. Kotowski A (ed) (1954) Gmelins Handbuch der anorganische Chemie, vol 62 (Gold). Verlag Chemie, Weinheim, p 716
25. Bailar JC, Emeléus HJ, Nyholm R, Trotman-Dickensen AF (eds) (1973) Comprehensive inorganic chemistry, vol 3. Pergamon Press, Oxford New York, p 150
26. Inzelt G, Puskas Z, Nemeth K, Varga I (2005) J Solid State Electrochem 9:823. doi:10.1007/s10008-005-0019-5